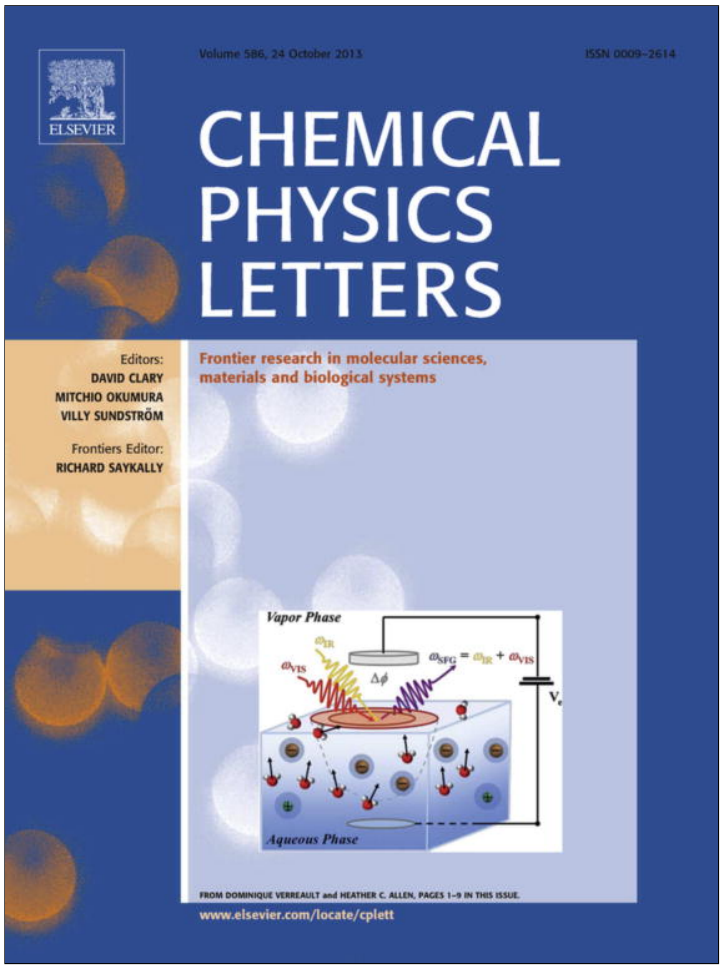

Chemical Physics Letters 586 (2013) 16–20

Contents lists available at ScienceDirect

Chemical Physics Letters

journal homepage: www.elsevier.com/locate/cplett

Polarisation labelling spectroscopy of the $D^1\Pi$ state in Na^7Li molecule

Nguyen Huy Bang [a,*], Dinh Xuan Khoa [a], Nguyen Tien Dung [a], J. Szczepkowski [b], W. Jastrzebski [b], P. Kowalczyk [c], A. Pashov [d]

[a] Vinh University, 182 Le Duan Str., Vinh City, Viet Nam
[b] Institute of Physics, Polish Academy of Sciences, Al.Lotników 32/46, 02-668 Warsaw, Poland
[c] Institute of Experimental Physics, Department of Physics, University of Warsaw, ul. Hoża 69, 00-681 Warsaw, Poland
[d] Department of Physics, Sofia University, 5 James Bourchier blvd., 1164 Sofia, Bulgaria

ARTICLE INFO

Article history:
Received 5 July 2013
In final form 2 September 2013
Available online 11 September 2013

ABSTRACT

We report the first experimental observation of the $D(2)^1\Pi$ state in the NaLi molecule. Polarisation labelling spectroscopy technique is applied to observe transitions to all vibrational levels in this state, save $v = 0$. The inverted perturbation approach method is used to construct a pointwise potential curve for the D state, which has a small barrier (9.3 cm^{-1}) to dissociation, located at 7.98 Å.

1. Introduction

The NaLi molecule for long time belonged to the least known heteronuclear alkali dimers. This resulted equally from problems with generating molecular vapour at high enough and stable concentration and from simultaneous presence of Na_2 and Li_2 molecules, both of which absorb light in the same spectral regions as NaLi. Until the beginning of this century only four electronic states have been characterised with spectroscopic accuracy: $X(1)^1\Sigma^+$, $A(2)^1\Sigma^+$, $B(1)^1\Pi$ and $C(3)^1\Sigma^+$ [1–3]. Over the last few years, using polarisation labelling spectroscopy (PLS) technique in combination with an efficient heat pipe source for production of mixed molecular vapour, we have been able to extend experimental investigations of NaLi to some higher lying electronic states. Examination of transitions from the ground $X^1\Sigma^+$ state to $E(4)^1\Sigma^+$, $3–7^1\Pi$, $5^1\Sigma^+$, $6^1\Sigma^+$ and $10^1\Sigma^+$ states at resolution better than 0.1 cm^{-1} led to analysis of the vibrational and rotational structure of these states and construction of corresponding potential energy curves [4–10]. Thus, among excited states accessible from the ground electronic state by absorption of one photon from the visible range, only the $D(2)^1\Pi$ state has so far escaped detection under rotational resolution. The sole experiment on this state, involving resonant two-photon ionization of NaLi, revealed positions of a few vibrational band heads in the $D^1\Pi \leftarrow X^1\Sigma^+$ system [11]. In the present work we have recorded rotationally resolved D ← X transition for the first time. The observed bound vibrational levels reach up to $v' = 16$, the highest level contained in the D state potential and a broad range of rotational quantum numbers, $J' = 1 - 57$, is covered. Spectroscopic constants are determined for the investigated state and the potential energy curve is constructed from the experimental data. The potential curve reveals a small rotationless barrier to dissociation, in agreement with theoretical predictions [12,13]. It can be noticed at this juncture that the interest in electronic structure of NaLi has recently increased due to successful experiments on production of cold molecules from an ultracold mixture of sodium and lithium [14–16].

2. Experiment

The experimental arrangement was similar to that employed in our previous investigations of NaLi [4,5]. In brief, vapour containing NaLi was produced by heating metallic sodium and lithium (natural isotopic composition) to about 670 and 880 K, respectively, in a dual-temperature heat-pipe oven [17]. A total pressure of 4 Torr was established in the oven using argon as a buffer gas. Known levels of the ground state of Na^7Li were labelled with light of a pulsed dye laser operated on DCM or DCM/Cresyl Violet mixture (home built in a grazing incidence configuration [18], linewidth below 0.5 cm^{-1}) and set on selected transitions in the A ← X band system of NaLi [2], preferably chosen to be off-resonance with any Na_2 or Li_2 transition. To control the labelling laser frequency a HighFinesse WS-7 wavemeter was employed. Alternatively, the ($v'' = 0, J'' = 30$) level could be labelled with light of a cw Ar^+ laser operated on the 496.5 nm line (40 mW power) [4]. Transitions from the labelled ground state levels to the investigated $D^1\Pi$ state were excited in a V-type optical–optical double resonance polarisation scheme, using pulsed light from a Lumonics HD500 dye laser delivering 5 mJ pulses of 0.05 cm^{-1} linewidth ('pump' laser). With POPOP, Stilben 2, Coumarin 440, 450 and 460 dyes we were able to scan the pump laser frequency over the spectral region 21550–24050 cm^{-1}, corresponding to the D ← X band system in NaLi. Both dye lasers were pumped by the same XeCl excimer laser (LightMachinery IPEX-848, 120 Hz

* Corresponding author.
E-mail address: nguyen@ifpan.edu.pl (N.H. Bang).

0009-2614/$ - see front matter © 2013 Published by Elsevier B.V.
http://dx.doi.org/10.1016/j.cplett.2013.09.003

repetition rate, 10 ns pulse duration) to ensure temporal coincidence of light pulses. Beams of the labelling and pump lasers were crossed at a small angle in the molecular sample. The intensity of the labelling beam was monitored through a polariser–analyser system (Glan-Thompson prisms placed either side of the heat-pipe) so that double resonance signals appeared on a black background. Calibration of the pump laser frequency during the scan was achieved by simultaneously recording the spectrum of argon and neon produced in optogalvanic cells and the fringes produced when part of the laser radiation was sampled by a 0.5 cm long Fabry-Pérot interferometer. The accuracy of frequency measurements was estimated to be better than 0.05 cm^{-1}, where the main error comes from the uncertainty of positions of the Ar and Ne optogalvanic lines [19].

3. Data analysis and results

As the spectral region under investigation is conveniently situated in a gap between two strong band systems of Na_2, B $\leftarrow$ X and C $\leftarrow$ X, we were able to observe clean spectra of NaLi. An example, with parts of the $D^1\Pi$ $(v',J') \leftarrow X^1\Sigma^+(v''=0,J''=5)$ and $D^1\Pi$ $(v',J') \leftarrow X^1\Sigma^+(v''=0,J''=17)$ progressions, is presented in Figure 1. The characteristic feature of the spectra was that all the recorded progressions terminated abruptly at $v' \leqslant 16$, independently of the starting v'' level, although the vibrational separations had not converged. This agrees with the theoretical prediction of a potential barrier in the D state. Altogether some 800 lines were identified as belonging to the D $\leftarrow$ X system, all in the Na^7Li isotopologue. The measured wave numbers of lines were converted to energies of D state levels referred to the bottom of the ground state potential well using the molecular constants of the $X^1\Sigma^+$ state [1], reproducing its level positions to 0.005 cm^{-1}. The uncertainty of the D state levels, therefore, comes mainly from the uncertainty of the measured line frequencies. Rotational quantum numbers J' were assigned basing on the knowledge of J'' in the labelled levels. Vibrational numbering in the D state was adopted from the low resolution experiment of Kappes et al. [11], who nevertheless was able to determine the absolute numbering on the basis of the isotope shift between Na^7Li and Na^6Li molecules. An access to the results of Ref. [11] was particularly important as due to unfavourable Franck-Condon factors we were not able to see the $v'=0$ level of the $D^1\Pi$ state in excitation spectra originating from

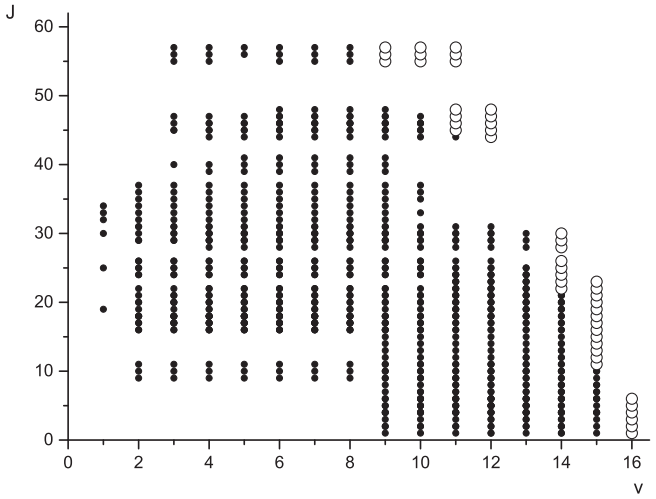

Figure 2. Distribution of the experimental data in the field of vibrational and rotational quantum numbers of the $D^1\Pi$ state in Na^7Li. Full circles correspond to levels included in the fit of Dunham coefficients, open points indicate additional levels used for construction of the IPA potential. Note that *e* and *f* parity levels corresponding to the same (v,J) quantum numbers are represented by single points.

$v''=0-2$ levels labelled in the present experiment and our own data start from $v'=1$. Distribution of the observed rovibrational levels is shown in Figure 2.

In the first stage of the analysis we tried to fit in a least squares sense all the experimentally determined energies of rovibrational levels in the $D^1\Pi$ state with the well known Dunham expansion

$$T(v,J) = \sum_{i,k} Y_{ik}(v+0.5)^i[J(J+1)-1]^k + \delta qJ(J+1). \quad (1)$$

where Y_{ik} are the Dunham coefficients, q is the lambda doubling constant and $\delta = 0$ or 1 corresponds to *f* levels which give rise to the Q lines or *e* levels giving rise to P and R lines, repectively. The fit was satisfactory for most of the observed rovibrational levels save those with the highest energies, see Figure 2, presumably located close to the top of the expected potential barrier. In the final analysis 17 coefficients were fitted to 566 observed D state levels. The standard error of the least squares fit was 0.06 cm^{-1}, which

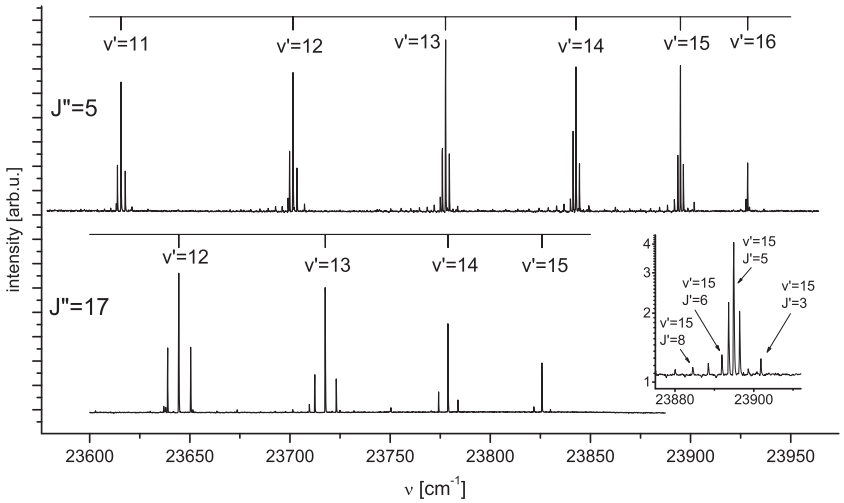

Figure 1. Two portions of the polarisation spectra of Na^7Li. The assigned progressions correspond to transitions $D^1\Pi$ $(v',J'=J''\pm1) \leftarrow X^1\Sigma^+(v'',J'')$ from the ground state levels $v''=0, J''=5$ (upper panel) labelled by the probe laser set at the wave number 15083.8 cm^{-1} and from $v''=0, J''=17$ (lower panel) labelled at 15565.4 cm^{-1}. An example of collisional satelites of the main Q transitions is displayed in the inset (note the logarithmic intensity scale there).

Table 1
The Dunham coefficients that describe the $D^1\Pi$ state of Na^7Li in the range of vibrational and rotational levels denoted by full circles in Figure 2. The number in parentheses that follows a quantity is the exponent of 10 that multiplies the quantity. The quoted error σ of a constant is one standard deviation. All numbers are in cm^{-1}.

constant	value	σ
T_e	22299.66	0.17
Y_{10}	148.867	0.127
Y_{20}	-0.46817	0.0354
Y_{30}	-0.21451	0.00447
Y_{40}	0.11278 (-1)	0.263 (-3)
Y_{50}	-0.35380 (-3)	0.580 (-5)
Y_{01}	0.221655	0.186 (-3)
Y_{11}	0.792 (-3)	0.150 (-3)
Y_{21}	-0.87031 (-3)	0.439 (-4)
Y_{31}	0.95619 (-4)	0.584 (-5)
Y_{41}	-0.59496 (-5)	0.3603 (-6)
Y_{51}	0.10231 (-6)	0.846 (-8)
Y_{02}	-0.2399 (-5)	0.34 (-7)
Y_{12}	0.230 (-6)	0.10 (-7)
Y_{22}	-0.4056 (-7)	0.74 (-9)
Y_{03}	-0.622 (-10)	0.47 (-11)
q	0.94 (-4)	0.5 (-5)

only slightly exceeds the precision of measurement. The Dunham coefficients obtained from the fit are given in Table 1. In general, more significant figures are listed than would apparently be justified by the determined standard error. However, in some cases the extra digits are necessary due to the effects of correlation between the different Dunham coefficients. The $D^1\Pi$ state is connected with the $Li(2^2S_{1/2})$ and $Na(3^2P_{1/2})$ atomic asymptote and already at this stage of the analysis we were able to determine its dissociation energy. The dissociation limit is located 24059.6 cm^{-1} above the minimum of the ground state potential well, as results from the experimental values of the $X^1\Sigma^+$ dissociation energy (7103.4 ± 1.0 cm^{-1}, an averaged value from two models discussed in Ref.[14]) and the atomic excitation energy $3^2P_{1/2}$- $3^2S_{1/2}$ of sodium (16956.17 cm^{-1} [20]). By using the measured term energy T_e of the D state from Table 1, we arrive at value of $D_e(D^1\Pi)$ = 1759.9 ± 1.5 cm^{-1}, where the uncertainty is mainly due to the error of $D_e(X^1\Sigma^+)$ and the estimated uncertainty of T_e (1 cm^{-1}).

It is interesting to note that the positions of (v',0) band heads listed by Kappes *et al.* [11] for both Na^7Li and Na^6Li are systematically shifted to the red by 2 to 5 cm^{-1} in comparison to the respective positions calculated from the molecular constants of the D and X states. The difference exceeds the measurement uncertainty quoted in Ref. [11] (±2 cm^{-1}). Taking into account that the vibrational bands in the B $\leftarrow$ X system are red shaded and that the actual band heads correspond to the weak R(1) lines, the discrepancy can be attributed to a wrong assignment of the band head positions in the low resolution spectra of Kappes et al. to the places where R and Q branches pile up together, shifted by a few wave numbers to the red.

The molecular constants in Table 1 were used to calculate a preliminary rotationless RKR potential curve of the $D^1\Pi$ state, for obvious reasons valid only up to $v' = 15$ where the last rotational levels unaffected by the barrier ($J' = 1 - 10$) were found. To construct a molecular potential correctly representing the barrier and to make use of 57 observed highest energy levels excluded from the Dunham analysis, we used the Inverted Perturbation Approach (IPA) method in which the short range potential (for $R < R_{out}$) is represented by a set of grid points $[R_i, U_i]$ whereas in the long range an analytical expression

$$U_{LR}(R) = U_\infty - C_6/R^6 - C_8/R^8 - C_{10}/R^{10} \qquad \text{for } R > R_{out} \qquad (2)$$

is employed [21,22]. In general, the values U_i, C_n, U_∞ and R_{out} are fitting parameters to be adjusted in such a way that the difference between the measured level energies and their counterparts calculated from the molecular potential is minimum in a least squares sense. The IPA fitting routine requires a reasonable starting potential to be improved in subsequent iterations. For this purpose we used a hybrid potential based on the RKR curve in the inner part, extended by a barrier of a shape adopted from the theoretical D state potential of Mabrouk and Berriche [13] and, beyond the barrier, converging to the atomic limit according to Eq. (2). In the long range part we fixed the dissociation limit at its experimental value $U_\infty = 24059.6\ cm^{-1}$. As an initial guess of the dispersion coefficients C_6 and C_8 we took the theoretical values of Bussery et al. [23], resulting from the only calculations which take into account the fine structure splitting of the $2^2S + 3^2P$ atomic asymptote (Table 10 in their work). Since numerical tests have shown high correlation of C_6 and C_8, we decided to fix C_6 at the theoretical value and to fit C_8. The C_{10} coefficient and the point of connection R_{out} were also fitted to ensure a smooth matching of the long range part with the pointwise potential describing the inner part of the curve (for details of the procedure see Ref.[24]). Since the experimental data do not reach the region of the potential where the long-range expression (2) is valid, the parameters C_8 and C_{10} are only effective parameters and should not be compared with the theoretical calculations.

The quality of the preliminary fit using the Dunham expansion suggested not only that our model should take into account the presence of the potential barrier, but also that it might be necessary to include a dependence of the Λ doubling on the vibrational and rotational quantum numbers. Therefore, the q parameter, describing the shift of the e parity levels from the "unperturbed" f levels, was fitted either as a single constant (similarly as in the Dunham fit) or as a function $q(v,J) = q_0 + q_1 \cdot v + q_2 \cdot J(J+1)$. Both approaches resulted in a similar quality of the fit (rms = 0.029 cm^{-1}). All coefficients, q_0, q_1 and q_2 had statistically significant values. However, by studying the residuals of both fits, we did not observe any systematic deviation which would make one of the models more preferable. Therefore we decided to choose the simpler model, with a constant value of q. This result is rather unexpected and indicates a strong correlation between the shape of the potential curve and the q parameter for the present body of experimental data. Keeping in mind the experimental uncertainty and the missing information on the bottom of the potential curve, more accurate data and/or more measurements related to $v = 0, v = 1$ and $J > 60$ levels may help in the future to find the proper description of the Λ doubling of the D state in NaLi.

The final potential curve, based on 261 rovibrational levels of f parity and 360 e parity levels, is defined in the range 2 Å $\leqslant R \leqslant$ 11.92928 Å by 37 parameters $U(R)$ and for $R >$ 11.92928 Å by 4 long range parameters $[U_\infty, C_n]$, all of them listed in Table 2. The effect of the Λ doubling, as discussed above, has been taken into account by adding a correction $qJ(J+1)$ to energies of the e parity levels and the fitted value of q is also given in Table 2. In order to calculate the potential energy for an arbitrary internuclear distance between 2 Å and R_{out}, a natural cubic spline interpolation [25] through all 37 points of the short range potential should be applied. Actually points $U(R)$ given in the upper part of Table 2 extend up to 16 Å. Due to properties of cubic spline interpolation all of them are needed to calculate the potential energy curve but we stress that this curve is valid only at internuclear distances below the connection point R_{out}. For $R >$ 11.92928 Å long range expression (2) should be solely used for calculation of the potential energy. The presented potential reproduces the measured term energies of rovibrational levels in the $D(2)^1\Pi$ state used for its construction with a standard deviation 0.029 cm^{-1} if the Schrödinger equation is solved in a mesh of at least 7000 points between 2 and 16 Å. Histograms of the residuals from the fit are given in the Supplementary material. The f parity levels fit somewhat better

Table 2
Parameters defining the IPA potential energy curve of the $D^1\Pi$ state of NaLi.

R (Å)	U (cm^{-1})	R (Å)	U (cm^{-1})
2.0	34823.8882	3.9	22333.1360
2.1	33119.5763	4.0	22395.1989
2.2	31371.8651	4.1	22483.6399
2.3	29719.2695	4.2	22590.8287
2.4	28348.6429	4.4	22834.8481
2.5	27167.4940	4.6	23084.1882
2.6	26176.3919	4.8	23311.9381
2.7	25347.6186	5.0	23505.3076
2.8	24655.4021	5.2	23661.1771
2.9	24111.3227	5.4	23781.7714
3.0	23650.2503	5.6	23872.6004
3.1	23266.4208	5.8	23938.3475
3.2	22965.2520	6.2	24018.6258
3.3	22729.4579	7.1	24065.9534
3.4	22552.3012	8.6	24068.1703
3.5	22426.0730	10.1	24065.9715
3.6	22346.0999	12.4	24062.9823
3.7	22306.4918	16.0	24061.1800
3.8	22302.8516		
$q = 8.252 \cdot 10^{-5}$ cm^{-1}			
$R_{out} = 11.92928$ Å			
$U_\infty = 24059.6$ cm^{-1}			
$C_6 = -2.538 \cdot 10^7$ $cm^{-1}Å^6$		$C_8 = 1.902 \cdot 10^9$ $cm^{-1}Å^8$	
$C_{10} = 1.566 \cdot 10^{10}$ $cm^{-1}Å^{10}$			
Calculated parameters:			
$T_e = 22299.93$ cm^{-1}		$R_e = 3.7595$ Å	

to the model (rms 0.028 cm^{-1}) than the e levels (rms 0.030 cm^{-1}). For only 7 levels deviations exceed 2σ. Small systematic deviations (less than 1σ) may still be observed for higher J levels, and they cannot be avoided even when v and J dependent Λ doubling is fitted. We see several possible reasons for this. The missing observations for $v = 0$ and very few for $v = 1$ levels make the determination of the potential minimum less safe. The situation is further complicated by the Λ doubling and possibly by other second order effects, which seem quite regular on the present level of experimental uncertainty. We believe that the discussion on methods of better description of the D state should be postponed until more experimental data are collected.

4. Discussion

The $D^1\Pi$ state has been a subject of two recent calculations [12,13] and the salient molecular constants determined in the present work can be compared with those predicted theoretically (Table 3). Petsalakis et al. [12] published only a limited set of molecular parameters; their potential curve is located too low and is much too shallow. The constants of Mabrouk and Berriche [13] are in remarkable agreement with the experimental ones, except of ω_e. The exact coincidence of their T_e value with the measured term energy of the D state is rather fortuitous, because the difference in dissociation energies shows that the calculated position of the atomic asymptote is actually off by a few tens of cm^{-1}. To explore the accuracy of calculations of Ref. [13] we took a closer

Table 3
Comparison of the experimental and theoretical molecular constants of the $D^1\Pi$ state of Na^7Li (values in cm^{-1}, except for R_e in Å). In parentheses the experimental errors are given in units of the last digits.

	This work	Ref. [12]	Ref. [13]
T_e	22300(1)	21895	22300
D_e	1759.9(1.5)	1450	1722
ω_e	148.87(13)		155.25
B_e	0.2217(2)		0.2260
R_e	3.761(2)	3.82	3.725

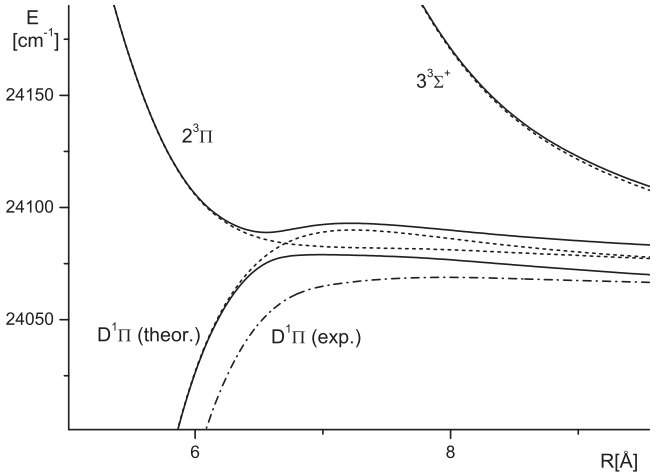

Figure 3. Comparison of the potential barrier constructed from the experimental data (dash - dot line) with the theoretical predictions of Ref. [13] neglecting spin-orbit coupling (dashed lines) and with the related $\Omega = 1$ potential curves obtained in an approximate model described in the text (solid lines).

look at the shape of the potential barrier (Figure 3). For a direct comparison of potentials at energies around the dissociation limit, positions of the asymptotes have to be matched correctly. Here we have to note that the calculation neglects the spin-orbit splitting of the atomic asymptote and the theoretical curve [13] converges to the centre of gravity of the $Li(2^2S_{1/2})$+ $Na(3^2P_J)$ manifold, situated 11.5 cm^{-1} above the actual D state dissociation limit. However, we can still juxtapose the barrier heights and positions of the maxima, which are 9.3 cm^{-1}, 7.96 Å and 17.0 cm^{-1}, 7.24 Å for the experimental and theoretical potentials, respectively. Figure 3 might suggest that the excessive height of the calculated barrier is due to neglect of influence of the $2^3\Pi$ state on the shape of the D state potential in Hund's case (a). Actually, the spin-orbit interaction couples the $D^1\Pi$ state with $\Omega = 1$ components of the $2^3\Pi$ and $3^3\Sigma^+$ states (see Figure 3) and and the Hund's case (c) is more appropriate for description of all three states at energies close to the atomic asymptote. In approximation which assumes independence of molecular spin-orbit interaction from internuclear distance, the transition case (a) → case (c) can be accomplished by diagonalization of the following Hamiltonian matrix [26]:

$$\begin{pmatrix} U(D^1\Pi) & -A/2 & A/2 \\ -A/2 & U(2^3\Pi) & A/2 \\ A/2 & A/2 & U(3^3\Sigma^+) \end{pmatrix}$$

where $U(D^1\Pi)$, $U(2^3\Pi)$ and $U(3^3\Sigma^+)$ correspond to the respective potential curves in Hund's case (a) and A stands for the atomic spin–orbit parameter for $Na(3^2P)$

$$A = \frac{2}{3} \cdot [E(3^2P_{3/2}) - E(3^2P_{1/2})] = 11.5 \text{ cm}^{-1}. \quad (4)$$

With the case (a) potentials taken from calculations by Mabrouk and Berriche [13] we obtained in this model the potential energy curves displayed in Figure 3 by solid lines. An apparent lowering of the barrier is deceptive because, simultaneously, the dissociation limit of the D state is pushed down to its correct position, i.e. the $Li(2^2S_{1/2})$ + $Na(3^2P_{1/2})$ asymptote. The net result is nearly negligible for the barrier height (now equal to 17.3 cm^{-1}) and only the position of the barrier maximum (6.98 Å) is influenced, however providing larger discrepancy between the experimental and theoretical values.

The last question to be discussed is up to what internuclear distance is the experimentally derived potential reliable. For the last

observed level $v = 16$, $J = 6$ the outer turning point is $R_{out} = 7.1$ Å. Our data include several quasibound levels above the asymptote (the barrier region begins beyond 6.8 Å). However, at the resolution of our experiment, none of the transitions to these levels was measurably broadened. Therefore only the inner wall of the barrier is well characterised by the present measurements. The asymptotic behaviour of the potential is not really known and the leading long range coefficient C_6 cannot be determined by this analysis. It should be noted that the constructed potential supports four additional rotational levels for $v = 16$, i.e. $J = 7 - 10$. We believe that their increasing widths, predicted to vary between 0.3 cm^{-1} at $J = 7$ to 1 cm^{-1} at $J = 10$, made them unobservable in the present experiment.

The financial support of the Vietnamese team from the Vietnam's National Foundation for Science and Technology Development (NAFOSTED) under the project code 103.06.110.09 is acknowledged. J.S., W.J. and P.K. were partially supported by the Polish Ministry of Science and Higher Education through grant No. N202 203938.

Appendix A. Supplementary data

Supplementary data associated with this letter can be found, in the online version, at http://dx.doi.org/10.1016/j.cplett.2013.09.003. They are also deposited at the web page http://dimer.ifpan.edu.pl.

References

[1] C.E. Fellows, J. Chem. Phys. 94 (1991) 5855.
[2] C.E. Fellows, J. Mol. Spectrosc. 136 (1989) 369.
[3] C.E. Fellows, J. Vergès, C. Amiot, J. Chem. Phys. 93 (1990) 6281.
[4] W. Jastrzebski, P. Kowalczyk, R. Nadyak, A. Pashov, Spectrochim. Acta A 58 (2002) 2193.
[5] Nguyen Huy Bang, W. Jastrzebski, P. Kowalczyk, J. Mol. Spectrosc. 233 (2005) 290.
[6] Nguyen Huy Bang, A. Grochola, W. Jastrzebski, P. Kowalczyk, Chem. Phys. Lett. 440 (2007) 199.
[7] Nguyen Huy Bang, A. Grochola, W. Jastrzebski, P. Kowalczyk, J. Chem. Phys. 130 (2009) art. no. 124307.
[8] I.D. Petsalakis, G. Theodorakopoulos, A. Grochola, P. Kowalczyk, W. Jastrzebski, Chem. Phys. 362 (2009) 130.
[9] W. Jastrzebski, P. Kowalczyk, A. Pashov, J. Szczepkowski, Spectrochim. Acta A 73 (2009) 117.
[10] Nguyen Huy Bang, A. Grochola, W. Jastrzebski, P. Kowalczyk, Opt. Mater. 31 (2009) 527.
[11] M.M. Kappes, K.O. Marti, P. Radi, M. Schär, E. Schumacher, Chem. Phys. Lett. 107 (1984) 6.
[12] I.D. Petsalakis, D. Tzeli, G. Theodorakopoulos, J. Chem. Phys. 129 (2008) art. no. 054306.
[13] N. Mabrouk, H. Berriche, J. Phys. B 41 (2008) art. no. 155101.
[14] M. Steinke, H. Knöckel, E. Tiemann, Phys. Rev. A 85 (2012) art. no. 042720.
[15] T. Schuster, R. Scelle, A. Trautmann, S. Knoop, M.K. Oberthaler, M.M. Haverhals, M.R. Goosen, S.J.J.M.F. Kokkelmans, E. Tiemann, Phys. Rev. A 85 (2012) art. no. 042721.
[16] M.-S. Heo, T.T. Wang, C.A. Christensen, T.M. Rvachov, D.A. Cotta, J.-H. Choi, Y.-R. Lee, W. Ketterle, Phys. Rev. A 86 (2012) art. no. 021602(R).
[17] V. Bednarska, I. Jackowska, W. Jastrzębski, P. Kowalczyk, Meas. Sci. Technol. 7 (1996) 1291.
[18] I. Shoshan, N.N. Danon, U.P. Oppenheim, J. Appl. Phys. 48 (1977) 4495.
[19] A.R. Striganov, G.A. Odincova, Tablicy Spektralnych Linii Atomov i Ionov, Energoizdat, Moscow, 1982.
[20] J.E. Sansonetti, J. Phys. Chem. Ref. Data 37 (2008) 1659.
[21] A. Pashov, W. Jastrzebski, P. Kowalczyk, Comput. Phys. Commun. 128 (2000) 622.
[22] A. Pashov, W. Jastrzebski, P. Kortyka and P. Kowalczyk, J. Chem. Phys. 124 (2006) art. no. 204308.
[23] B. Bussery, Y. Achkar, M. Aubert-Frécon, Chem. Phys. 116 (1987) 319.
[24] O. Allard, C. Samuelis, A. Pashov, H. Knöckel, E. Tiemann, Eur. Phys. J.D 26 (2003) 155.
[25] C. DeBoor, A Practical Guide to Splines, Springer, Berlin, 1978.
[26] T. Bergeman, P.S. Julienne, C.J. Williams, E. Tiesinga, M.R. Manaa, H. Wang, P.L. Gould, W.C. Stwalley, J. Chem. Phys. 117 (2002) 7491.